Charge transport and Photo-response Study of Methylammonium Lead Bromide based Heterojunction Device

Jyoti Chaudhary[1], Chandra Mohan Singh Negi [2], Varsha Yadav[1], Saral K. Gupta[1], Ajay Singh Verma[1 a)]

[1]*Department of Physics, Banasthali Vidyapith, Banasthali 304022, INDIA*
[2]*Department of Electronics, Banasthali Vidyapith, Banasthali 304022, INDIA*
a) Corresponding author: ajay_phy@rediffmail.com

Abstract. In this work, we report the fabrication and characterization of Methylammonium lead bromide ($CH_3NH_3PbBr_3$) based Heterojunction device. Surface morphology of the $CH_3NH_3PbBr_3$ film prepared using spin coating technique was assessed using field emission scanning electron microscope (FESEM). The measured current-voltage (I-V) characteristic of the device was analyzed to evaluate the various diode parameters and understand the charge transport properties. Analysis of space charge limited conduction (SCLC) region of the charge transport indicates the carrier mobility of $1.59\times10^{-4}cm^2V^{-1}s^{-1}$. The current level in the device increases considerably under light excitation. Furthermore, impedance spectroscopy analysis was performed to identify the internal circuit parameters of the device.

INTRODUCTION

Hybrid halide perovskites have been emerging as a wonderful material for photovoltaic and optoelectronic applications, they are in position to replace the silicon solar cells technology very soon. Organo-metal trihalide perovskites have attracted considerable attention around the globe for application in solar cells and other electronic devices due to their effective efficiency, flexibility and very cheap cost for production [1-3]. Recent studies show that halide perovskites have shown enormous potential to become the perfect candidate in photovoltaic devices with their outstanding properties, including good charge transportation, eminent absorption coefficient, and long diffusion length, which make them excellent active layer material for photovoltaic/optoelectronic devices[4-5].

In the perovskite family, Methylammonium lead iodide ($CH_3NH_3PbI_3$) is the most widely studied material, in contrast to this tri-iodide counterpart Methylammonium lead bromide ($CH_3NH_3PbBr_3$) received little attention. Recently, $CH_3NH_3PbBr_3$ is have been vigorously investigated for a variety of applications, ranging from tandem solar cells to light emitting diodes [1-2]. Nevertheless, the fundamental aspects of devices based on $CH_3NH_3PbBr_3$, such as charge transport mechanism has been rarely studied.

Herein, planar $CH_3NH_3PbBr_3$based device were fabricated using a spin-coating method on fluorine tin oxide (FTO) coated glass substrate. Perovskite based devices are mostly fabricated with three vital units, that is, electron transport layer (ETL), perovskite layers (active layer), and hole transport-layer (HTL) [7-9].We have prepared a multi-layer structure consists of FTO/titanium oxide (TiO_2)/$CH_3NH_3PbBr_3$/poly (3,4-ethylenedioxythiophene) polystyrene sulfonate (PEDOT:PSS)/ aluminum (Al). This study focuses on the surface and electrical properties of the $CH_3NH_3PbBr_3$ films and based devices. The fabricated device was characterized by DC current-voltage (I-V) characteristics and electrical impedance spectroscopy (EIS) technique.

EXPERIMENTAL DETAILS

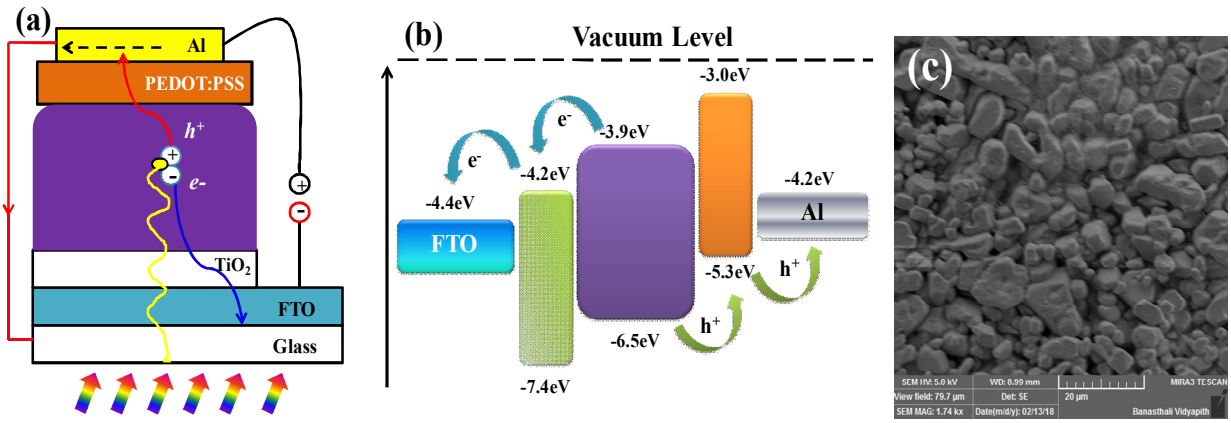

FIGURE 1. (a) Energy level sketch of materials used in the fabrication of device, **(b)** schematic device structure of the perovskite based device, **(c)** FESEM image of $CH_3NH_3PbBr_3$ perovskites film.

CH_3NH_2 has been mixed with HBr with the help of magnetic stirring. The resulting mixture has been heated to evaporate the solvent. The obtained material (CH_3NH_3Br) has been washed 3 times in di-ethyl-ether and dried in vacuum oven. Thereafter, Methylammonium lead bromide ($CH_3NH_3PbBr_3$) has been incorporated in dimethyl-formamide (DMF) to form the perovskite nanoparticles ($CH_3NH_3PbBr_3$). For device fabrication, firstly TiO_2 precursor solution was deposited on FTO substrate at 4000 rpm for 40 s by spin-coated technique to deposit a thin film of electron transport layer (ETL). After that the substrate was annealed at 125°C for 10 minutes and placed in furnace for sintering at 500 °C for 45 minutes. $CH_3NH_3PbBr_3$ precursor solution was then dispensed ontoTiO_2 layer to fabricate the active layer. Then a hole transport layer of $PC_{61}BM$ was deposited at 2500 RPM for 40sover active layer. Finally, Al has been evaporated by using thermal evaporation technique at a pressure of 10^{-5}torrto form the top electrode of device. The resulting device structure and energy level diagrams of the materials used for fabrication of devices are shown in figure 1 (a) and 1(b), respectively. To evaluate the device performance, the fabricated device has been characterized by using electrical techniques such as I-V and impedance spectroscopy (IS).

RESULTS AND DISCUSSION

The FESEM image of $CH_3NH_3PbBr_3$ deposited over FTO coated glass substrate shown in Fig. 1 (c) reveal uniform perovskite film with entire surface coverage [10]. The measured I-V characteristic of the device under illumination and dark condition is displayed in Fig. 2(a). The current increases exponentially in forward bias under dark condition, while in reverse bias current is nearly independent of the applied voltage. Under illumination condition, current levels increases as compared to dark current, this indicates the device exhibits the photoconductive behavior. The electron hole pairs generated by excitation of the light are drifted towards the respective electrode under the control of the applied electric field, results into the generation of photocurrent in the device. The diode parameters are extracted from the semi logarithmic curve shown in Fig. 2(b) in the framework of thermionic emission theory [11]. The evaluated values of ideality factor, barrier height and saturation current at room temperature are 3.4, 0.64 eV and $8.1X10^{-4}$A, respectively.

To recognize the current conduction mechanism, the I-V characteristics curve is re-plotted in double logarithmic scale and fitted with the power law curve ($I \alpha V^m$), as shown in figure 2 (c). Here m represents the slope of the curve and distinguish the different conduction mechanisms. The slope in the low voltage region is close to 1, implying that the current conduction mechanism at low voltage is of Ohmic nature. The slope turn into 4.3 at mid-voltage region, representing trap controlled space charge limited conduction (TCLC) mechanism. In this voltage range, current is limited by the space charge formed in the active layer in the presence of traps within the forbidden gap of the perovskite. The injected charge carrier unable to transport as fast as they are injected from the electrode

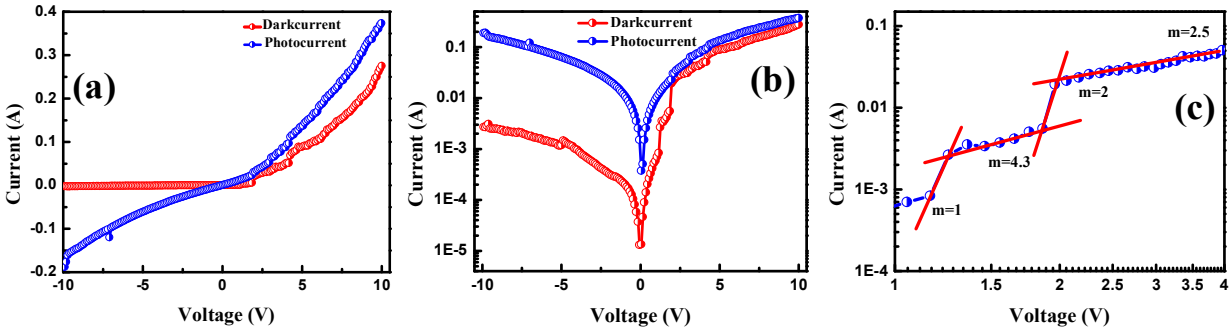

FIGURE 2: FTO/TiO_2/$CH_3NH_3PbBr_3$/PEDOT:PSS/Al **(a)** I-V characteristics of the perovskite device in dark &light, **(b)** I-V characteristic in semi logarithmic scale of device, **(c)** double-logarithmic plot of the device.

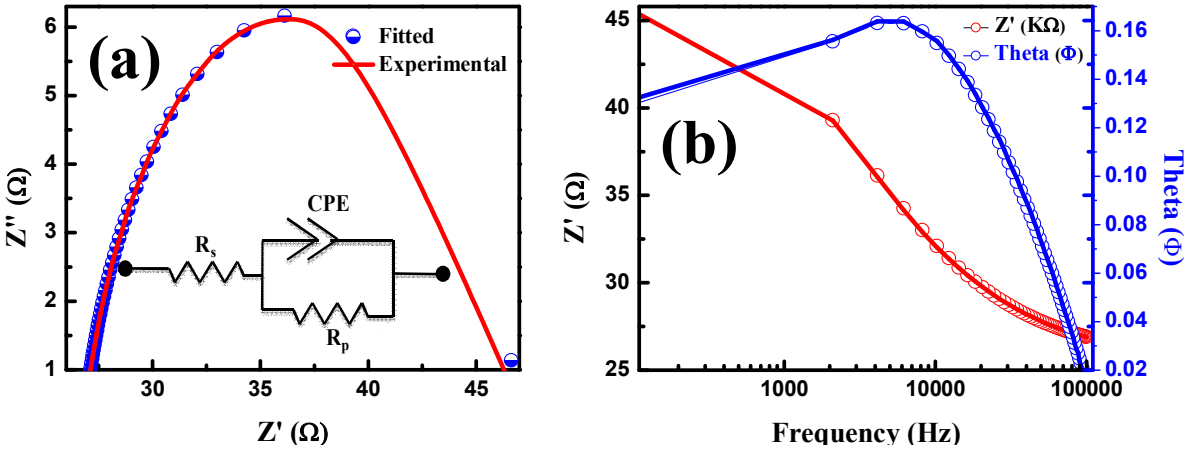

FIGURE 3. (a) Nyquist plot of the device under study, inset shows electrical equivalent circuit of the device, **(b)** Bode plots of the device in dark condition.

into the perovskite layer, causing accumulation of charge carrier, thus formation of the space charge layer near the injecting electrode, that impede further injection process, limiting the current flow in the device. However, in the presence of traps, the accumulated charge carriers might excited to the traps, which allow the further injection of carrier, resulting in the rapid change of the current with applied voltage, as represented by the slope 4.3 in the Fig. 2 (c).At large voltage region, slope changes to 2, which is the symptom of space limited charge conduction (SCLC) mechanism. Since all traps are acquired by the charges, so space charge again start forming in the perovskite layer, therefore current exhibits the SCLC behavior. By applying Mott-Gurney's law in SCLC region, the electron mobility in the device is found to be $1.59\times10^{-4}cm^2V^{-1}s^{-1}$.

Furthermore, electrochemical impedance spectroscopy (EIS) was carried out at 0 Volt DC to enumerate the internal circuit parameters of the device, such as series resistance, space charge capacitance and leakage resistance. The measured results are fitted with the simulated results and plotted in Figure 3. The simulated results are acquired using the appropriate electrical equivalent circuit, as shown in the inset of Fig. 3(a). As can be apparent from the figures, experimental results are good matched with the simulated results. The equivalent circuit comprises of parallel combination of leakage resistance (R_p) and constant phase element (CPE) in series with the series resistance R_s. The CPE is used as an alternative of pure capacitor to obtain the good match between experimental and simulated data, which implies the non-uniformity of the junction. Nevertheless, the capacitance can be easily calculated from CPE by the relation $Cp= (R_pY_o)^{1/n}/R_p$, where, Cp represent the space charge capacitance, and Y_o and the parameters related to the CPE [12]. The extracted parameters; Rs, Rp and Cp are found to be 18.70 Ω, 26.77 Ω and 16.9 μF, respectively. The rise time of the device can be determined from the relation τ_r=2.2 RXC and the value comes out to be equal to $9.92X10^{-4}$ s.

CONCLUSIONS

The Heterojunction device of the architecture FTO/TiO_2/$CH_3NH_3PbBr_3$/PEDOT:PSS/Al was fabricated using spin-coating technique. The morphological study show uniform deposition of the $CH_3NH_3PbBr_3$ over the glass substrate. Electrical charactertics of device was analyzed by I-V and impedance measurements. Analysis of forward bias semi-logarithmic I-V curves show that the device exhibits the barrier height of 0.64, ideality factor of 3.4 and reverses saturation current of $8.1X10^{-4}$A. The charge transport properties of the device studied under the circumstance of SCLC depicts three distinct voltage dependent regions and enable us to extract the mobility of charge carrier. The higher value of current under light illumination compared to dark implies device show good photoresponse behavior. Finally, impedance study was undertaken to understand the internal electrical structure of device.

ACKNOWLEDGEMENTS

The authors are grateful to the Department of Science and Technology (DST) for providing the financial support from under the CURIE program (grant No. SR/CURIE- Phase-III/01/2015(G)), and MHRD FAST program (grant No.5-5/2014-TS.VII), Govt. of India.

REFERENCES

1. Sheng, R., Ho-Baillie, A. W., Huang, S., Keevers, M., Hao, X., Jiang, L., Cheng, Y. B., & Green, M. A. (2015). Four-terminal tandem solar cells using $CH_3NH_3PbBr_3$ by spectrum splitting. The journal of physical chemistry letters, **6**, 3931-3934.

2. Shi, Z. F., Sun, X. G., Wu, D., Xu, T. T., Zhuang, S. W., Tian, Y. T., Li, X. J., & Du, G. T. (2016). High-performance planar green light-emitting diodes based on a PEDOT: PSS/$CH_3NH_3PbBr_3$/ZnO sandwich structure. Nanoscale, **8** 10035-10042.

3. M.Ye, X.Liu, J.Iocozzia, X.Liuand Z.Lin, Nanomaterials for Sustainable Energy (Springer, Cham 2016) pp. 1-39.

4. J. Liu, G. Wang, K. Luo, X. He, Q. Ye, C. Liao and J. Mei, Chem. Phys. Chem, **18** 617-625 (2017).

5. L. C. Chen, Z. L. Tseng, J. K. Huang, C. C. Chen and S. H. Chang, Coatings, **6** 53 (2016).

6. G. Lu, F. He, S. Pang, H. Yang, D. Chen, J. Chang and C. Zhang, Int. J. Photoenergy, Article ID 2562968 (2017).

7. Y. Liu, S. Ji, S. Li, W. He, K. Wang, H. Hu, and C. Ye, J. Mater. Chem. A, **3** 14902-14909 (2015).

8. Z. Zhu, Q. Xue, H. He, K. Jiang, Z. Hu, Y. Bai, and H. Ade, Advanced Sci. **3**1500353 (2016).

9. Q. Dong, Y. Fang, Y. Shao, P. Mulligan, J. Qiu, L. Cao and J. Huang, Science, aaa5760 (2015).

10. W. Wang, Z. Zhang, Y. Cai, J. Chen, J. Wang, R. Huang, X. Lu, X. Gao, L. Shui, S. Wu and J-M Liu, Nanoscale Res. Letts., **11** 316 (2016).

11. K. Harada, A. G. Werner, M. Pfeiffer, C. J. Bloom, C. M. Elliott, and K. Leo, Phys. Rev. Letts., **94** 036601(2005).

12. Raga, S. R., & Qi, Y. (2016). The effect of impurities on the impedance spectroscopy response of $CH_3NH_3PbI_3$ perovskite solar cells. The Journal of Physical Chemistry C, **120**, 28519-28526.